Coupled systems with quasi-periodic and chaotic dynamics

Alexander P. Kuznetsov[1], Yuliya V. Sedova[1], Nataliya V. Stankevich[1,2]

[1] Kotel'nikov's Institute of Radio-Engineering and Electronics of Russian Academy of Sciences, Saratov Branch, Zelenaya 38, Saratov, 410019, Russian Federation

[2] Laboratory of Topological Methods in Dynamics, National Research University Higher School of Economics, Bolshaya Pecherskaya str., 25/12, Nizhny Novgorod 603155, Russia

The interaction of a system with quasi-periodic autonomous dynamics and a chaotic Rössler system is studied. We have shown that with the growth of the coupling, regimes of two-frequency and three-frequency quasiperiodicity, a periodic regime and a regime of oscillation death sequentially arise. With a small coupling strength, doubling bifurcations of three-frequency tori are observed in the system. A chaotic regime, characterized by two additional zero Lyapunov exponents in spectrum, is revealed. Two-parameter Lyapunov exponent analysis and bifurcation analysis are presented. A new bifurcation scenario of transition from the regime of oscillation death to quasi-periodicity in coupled systems is described.

Keywords. Quasi-periodic oscillations, dynamical chaos, Rössler system, Lyapunov exponents, chaos with additional zero Lyapunov exponents

Introduction

The study of the interaction of self-oscillating systems is of great interest. It leads to a fundamental nonlinear phenomenon as like synchronization, which is widespread in physics, chemistry, biology, etc. [1-5]. There are three main classes of oscillating processes: periodic, quasi-periodic and chaotic. Synchronization of periodic self-oscillating systems was historically the first example of this kind. Its discovery dates back to the works of Huygens, and has now been investigated in details. Much later, ideas arose about the possibility of chaotic systems synchronization. By now, coupled chaotic systems have been studied quite fully [1-5]. As for the synchronization of quasi-periodic oscillations, this problem has been studied relatively recently [6-13]. From the point of view of physics, some progress in this direction has occurred due to the emergence of new examples of generators capable of demonstrating autonomous quasi-periodic oscillations. In general case, quasi-periodicity can be represented as oscillations characterized by the several incommensurable frequencies. For such oscillations attractor is a stable ergodic torus with dimension corresponding to number of incommensurable frequencies. Quasi-periodic oscillations are stable both in sense of Lyapunov and Poisson, but are non-periodic. By contrast,

almost periodic oscillations [14,15] are stable only in Poisson sense. Problems, such as the dynamics of autonomous generators, their experimental implementation, excitation of generators of this type by an external signal, dynamics of coupled generators were considered in [16-26]. Note that this topic is related to the fundamental problem of quasi-periodic bifurcations (bifurcations of invariant tori in the phase space), which still remains insufficiently studied [27–39].

When studying the interaction of oscillatory systems, the case of similar systems is traditionally considered, for example, the interaction of van der Pol oscillators with each other, Rössler systems with each other, etc. In a similar way, the problem of the dynamics of coupled quasi-periodic generators was introduced into consideration [20-22]. In applications, however, situations often arise that relate to the interaction of different types of subsystems. Such situations are still little studied. In this direction, one of the new examples is the case when the first subsystem can demonstrate autonomous quasi–periodic dynamics, and the second is chaotic oscillations. As a result of interaction of such kind heterogeneous systems, a new type of dynamical behavior containing features of both models can appear. We consider the relevant problems in the present paper. As the first subsystem we use the generator of quasi-periodic oscillations proposed and studied in [18, 19]. As the second chaotic subsystem, we use the traditional example – the Rössler system [1-2]. We describe a complete picture of possible dynamical regimes and bifurcations of such a system, and also show that, with a small coupling strength, the system can exhibit chaotic dynamics, but preserve multi-dimensional tori. In this formulation, the problem is quite general, and its results may be of importance for other cases as well. For example, well-known generators of chaotic oscillations can act as a second subsystem: the Anishchenko-Astakhov generator [40], the Chua circuit [41], etc.

The rest of the paper is structured as follows. In Section 2, we present object of investigation, discuss dynamics of autonomous quasi-periodic generator and Rössler system, and explain the way of coupling organization. We devote Section 3 to results of Lyapunov exponents analysis; demonstrate the possibility of different types of quasi-periodic regimes and chaos with additional two zero Lyapunov exponents. In Section 4, we describe results of numerical bifurcation analysis. We show a new route from area of oscillation death to quasiperiodicity.

2. Object of investigation

The equations of an individual generator capable of demonstrating autonomous quasi-periodic oscillations [20,21] have the form

$$\begin{aligned}\dot{x} &= y,\\ \dot{y} &= (\lambda + z + x^2 - \beta x^4)y - \omega_0^2 x,\\ \dot{z} &= b(\varepsilon - z) - ky^2.\end{aligned} \qquad (1)$$

Here x, y, z are dynamical variables, ω_0 is the natural frequency of the generator. The values of the other parameters are selected similarly to [20,21]: ε=4, b=1, k=0.02, β=1/18, λ=-1.

In oscillator (1) for the specified values of parameters in the range $6.2<\omega_0<8.4$, two-frequency quasi-periodic regimes 2T are observed, except for very narrow resonant intervals. Figure 1 shows the corresponding illustration in the form of a bifurcation tree[1]. It is constructed for the Poincaré section by a plane $\dot{x} = 0$, which corresponds to a set of points (x_s,0,z_s), and represents the dependence of the variable x_s on the frequency parameter ω_0. At the boundaries of the specified range of ω_0, the Neimark-Sacker bifurcations NS are realized, and outside it, the regime of the main limit cycle P is observed.

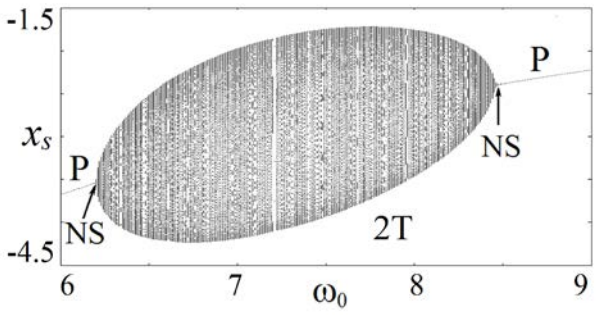

Fig.1. Bifurcation tree of an individual generator of quasi-periodic oscillations (1), ε=4, b=1, k=0.02, β=1/18, λ=-1. P is periodic oscillations (limit cycle); 2T is two-frequency quasi-periodic oscillations; NS is Neimark-Sacker bifurcation

As the second subsystem, we use the Rössler oscillator

$$\begin{aligned}\dot{x} &= -y - z,\\ \dot{y} &= x + py,\\ \dot{z} &= q + (x - r)z.\end{aligned} \qquad (2)$$

The values of the parameters are chosen equal to the traditional values p = 0.15, q = 0.4, r = 8.5 [1]. In this case, system (2) demonstrates chaotic dynamics.

Figure 2a shows the phase portrait of the generator (1) for the value of the parameter $\omega_0=2\pi$ corresponding to the case of quasi-periodic oscillations. In this case, a two-frequency invariant torus is implemented. Figure 2b shows the phase portrait of system (2), which is a classical chaotic Rössler attractor.

[1] For solution of ordinary differential equations in our numerical experiments, we used 4th order Runge-Kutta method with integration step 10^{-3}.

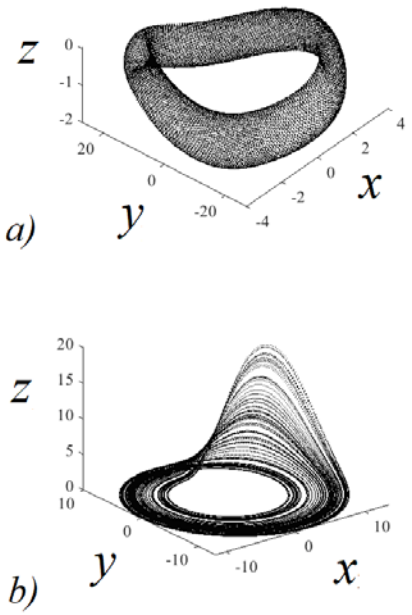

Fig.2. Phase portraits of the quasi-periodic generator (a), ε = 4, b = 1, k = 0.02, β = 1/18, λ = -1, $\omega_0 = 2\pi$, and the Rössler oscillator (b), p = 0.15, q = 0.4, r = 8.5.

Let us now write down the equations of the coupled systems (1) and (2):

$$\begin{aligned} &\dot{x}_1 = y_1, && \dot{x}_2 = -y_2 - z_2, \\ &\dot{y}_1 = (\lambda + z_1 + x_1^{\,2} - \beta x_1^{\,4}) y_1 - \omega_0^2 x_1 - \mu(\dot{x}_1 - \dot{x}_2), && \dot{y}_2 = x_2 + p y_2 + \mu(y_1 - y_2), \\ &\dot{z}_1 = b(\varepsilon - z_1) - k y_1^2, && \dot{z}_2 = q + (x_2 - r) z_2. \end{aligned} \qquad (3)$$

Here μ is the coupling parameter of subsystems. Let us briefly explain the introduction of coupling. As can be seen from (1), a quasi-periodic generator is a generalization of a van der Pol type oscillator. This is clearly seen if the variable z is discarded in the individual first subsystem. In this case, the coupling in the second equation through the velocity is dissipative, as for van der Pol oscillators [1, 2]. The same coupling is used in [22] for coupled quasi-periodic generators. For the Rössler oscillator, the coupling is introduced by analogy with [42-44] and is also dissipative. In particular, for two Rössler oscillators coupled in this way, a well-known effect of oscillation death is observed [1].

3. Analysis of Lyapunov exponents

3.1. One-parameter Lyapunov analysis

Let us now discuss the dynamics of system (3). We choose the value of the frequency parameter $\omega_0=2\pi$, which corresponds to the quasi-periodic dynamics in the individual first subsystem. Autonomous subsystems (1) and (2) demonstrate quasi-periodic and chaotic dynamics, respectively. In numerical simulations an appropriate criterion for distinguishing between these two types of behavior is the spectrum of Lyapunov exponents [45]. Lyapunov exponents characterize stability of close trajectories to infinitesimal perturbations. For 3-

dimensional subsystems a quasiperiodic attractor will be characterized by the spectrum: $\Lambda_1=\Lambda_2=0$, $\Lambda_3<0$, a chaotic attractor: $\Lambda_1>0$, $\Lambda_2=0$, $\Lambda_3<0$. In coupled systems (3) an attractor is characterized by six Lyapunov exponents, and it is possible to reveal a rich variety of quasi-periodic and chaotic attractors in accordance with the spectrum of Lyapunov exponents. In Table 1 we present possible dynamical regimes for 6-dimensional flow system in general case. Here we use "+" for designation of positive Lyapunov exponents, and "-" for negative, suggesting that they are sorted in descending order. Further we will use such classification.

Table 1. Possible types of dynamical regimes for 6-dimensional flow dynamical system in general case.

Dynamical regime	Λ_1	Λ_2	Λ_3	Λ_4	Λ_5	Λ_6
Stable equilibrium point	-	-	-	-	-	-
Periodic oscillations	0	-	-	-	-	-
Two-frequency quasiperiodic oscillations	0	0	-	-	-	-
Three-frequency quasiperiodic oscillations	0	0	0	-	-	-
Four-frequency quasiperiodic oscillations	0	0	0	0	-	-
Five-frequency quasiperiodic oscillations	0	0	0	0	0	-
Chaos	+	0	-	-	-	-
Hyperchaos	+	+	0	-	-	-
	+	+	+	0	-	-
	+	+	+	+	0	-
Chaos with additional zero Lyapunov exponents	+	0	0	-	-	-
	+	0	0	0	-	-
	+	0	0	0	0	-
Hyperchaos with additional zero Lyapunov exponents	+	+	0	0	-	-
	+	+	+	0	0	-
	+	+	0	0	0	-

Figure 3a shows graphs of the five Lyapunov exponents[2] of system (3) versus the coupling parameter in the range $0<\mu<0.25$[3]. The initial conditions were chosen to be fixed in the vicinity of the origin of coordinates in each of the subsystems ($x_{10}=0.02$, $y_{10}=0.01$, $z_{10}=0.03$, $x_{20}=0.01$, $y_{20}=0.03$, $z_{20}=0.02$).

Note that with zero coupling, the largest exponent is positive ($\Lambda_1>0$), since chaos is observed in the individual Rössler system. Also, for any coupling in self-oscillating regime, one of the exponents must be zero, which is necessarily for flow (continuous) systems.

[2] The spectrum of Lyapunov exponents was calculated according with algorithm described in [46] and using Gramm-Shmidt orthogonalisation.
[3] The sixth exponent is always negative.

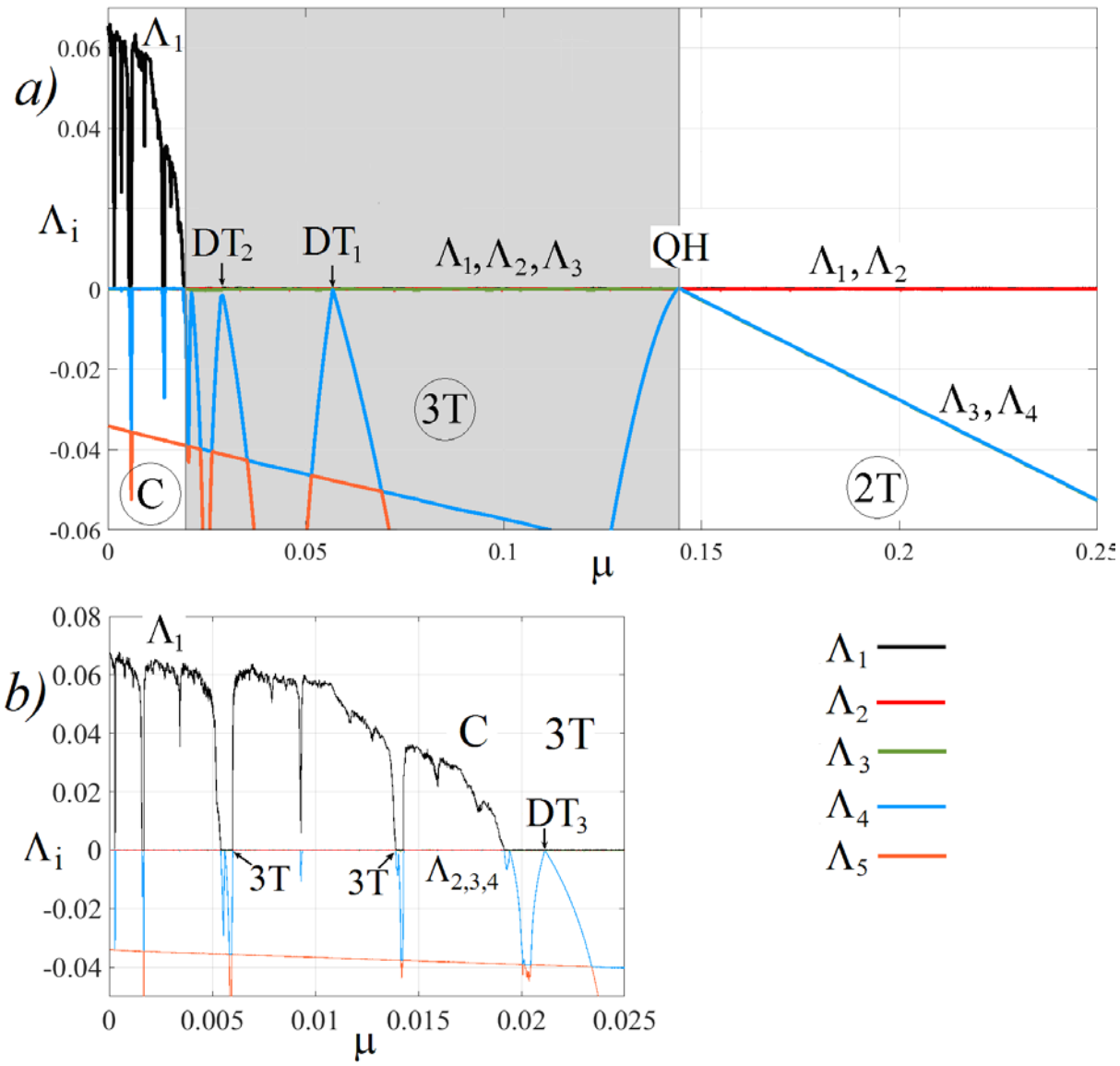

Fig.3. Graphs of Lyapunov exponents of coupled systems (3) depending on the coupling parameter. $DT_{1,2,3}$ are tori doubling bifurcations; QH is quasi-periodic Hopf bifurcation; 2T is two-frequency quasi-periodic oscillations; 3T is three-frequency quasi-periodic oscillations; C is chaos with two additional zero Lyapunov exponents

The graphs in Fig. 3a reveal three characteristic regions. In the case of a large coupling, the two largest exponents are zero ($\Lambda_1 = \Lambda_2 = 0$) and the rest are negative. Thus, a two-frequency invariant torus 2T is realized. As the coupling decreases, the exponents Λ_3, Λ_4 remain equal to each other, increase and turn to zero at the boundary of the 2T region. After that, the exponent Λ_3 remains zero, and Λ_4 again becomes negative. In accordance with the technique [28], this means that a quasi-periodic Hopf bifurcation QH occurs when a stable three-frequency torus 3T arises softly from a two-frequency torus. Inside the region 3T, three Lyapunov exponents are equal to zero ($\Lambda_1 = \Lambda_2 = \Lambda_3 = 0$), and the rest are negative. To improve visual perception, this area in Fig. 3a is shown with a gray fill.

As the coupling decreases, the three-frequency torus undergoes several doubling bifurcations DT, two of which are marked with arrows in Fig. 3a. In this case, the fourth exponent vanishes at the bifurcation point, remaining negative in its vicinity [28]. The Figure shows two such bifurcations DT_1 and DT_2.

In region C, the largest exponent becomes positive $\Lambda_1>0$, so that in general this is a region of chaos, and hyperchaos regimes with two positive exponents are not observed. For a more detailed analysis, let us turn to Fig. 3b, which shows an enlarged fragment of the Fig.3a in the coupling range $0<\mu<0.025$. In Fig. 3b, in the region of three-frequency tori, we can see one more (the third) doubling bifurcation of three-frequency torus DT_3.

The area in which the first exponent can be positive has the following features. First, for chaotic regimes three exponents turn to zero, so that $\Lambda_1>0$, $\Lambda_{2,3,4}=0$, $\Lambda_{5,6}<0$. Thus, chaos arises, characterized by three zero Lyapunov exponents (or very close to zero; the accuracy of zero Lyapunov exponent calculations is about 10^{-4}).

The possibility of chaos with one additional Lyapunov exponent was pointed out in [47, 48] at consideration the effect of a harmonic signal on a system with an autonomous quasi-periodicity Lorenz-84, simulating the long-term circulation of the atmosphere, as well as for an excited model map. Such an attractor was called the quasi-periodic Hénon attractor. It is the product of the Hénon attractor and the torus that leads to the formation of a chaotic attractor, which has a preserved saddle torus with two-dimensional neutral manifold in the flow (continuous) system. These examples [47, 48], however, refer to the case of one-side effect, while in systems with quasi-periodic dynamics the case of such effect forms an independent class [49]. Therefore, the emergence of new examples for mutually coupled flows is interesting. Some examples of this type have been noted in recent papers [22, 50, 51]. At the same time, this problem remains debatable, since there are no rigorous mathematical proofs, which is highlighted in [32]. In this regard, the authors of [52] say about “Lyapunov exponent very close to zero”, which can be indistinguishable from zero in numerical calculations. In our case, there is already a situation with two additional zero exponents, which is of some independent interest.

The second feature of Fig.3b consists in the fact that there are narrow windows in the chaos region where regimes of three-frequency tori originate. Two such windows are shown by arrows in Fig.3b.

3.2. Phase portraits

Figure 4 shows the phase portraits of the six-dimensional system (3) in projection onto the variables of the quasi-periodic generator and the Rössler system. The values of the coupling parameter are chosen in accordance with Fig.3, corresponding to chaos (a), three-frequency torus

(b), two-frequency torus (c). A portrait is also given for a significantly larger coupling μ=2.5 (d). For case (a), the coupling is very weak and the illustrations in the Figure are visually identical to ones for the individual subsystems in Fig.2. However, in fact, the six-dimensional system (3) demonstrates chaos, although the projections of the phase portrait on the subspaces of the subsystem variables look like a case of no coupling. During transition to the three-frequency torus (b), the portrait of the first subsystem practically does not change, and the portrait of the second subsystem noticeably differs from the Rössler chaotic attractor. This applies even more to the two-frequency torus (c). Finally, for a very large dissipative coupling, the torus turns out to "be suppressed", and both projections of attractors exhibit a limit cycle (d) corresponding to the periodic regime.

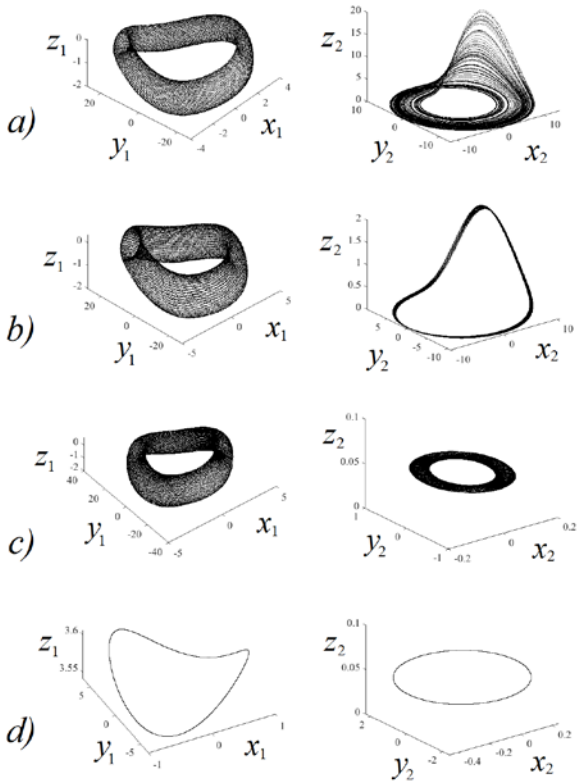

Fig.4. Evolution of phase portraits of subsystems with increasing coupling: (*a*) chaos with two additional zero Lyapunov exponents, μ = 0.002; (*b*) three-frequency quasi-periodic oscillations, μ = 0.1; (*c*) two-frequency quasi-periodic oscillations, μ = 0.2; (*d*) periodic oscillations, μ=2.5

Figure 5 shows the projections of bifurcation trees on the dynamical variables of each of the subsystems of the model (3), for the variable of the quasi-periodic generator (Fig. 5a) and for the variable of the Rössler system (Fig. 5b). The point of the quasi-periodic Hopf bifurcation QH is clearly visible on the trees, when, with a decrease in coupling, the two-frequency torus transforms into a three-frequency one. Figure 5a illustrates the soft nature of this bifurcation. Note that for the variable of the Rössler oscillator in Fig. 5b, to the right of the quasi-periodic bifurcation point QH, the region of the two-frequency torus is perceived as a thin line. In fact,

this branch of the tree corresponds to quasi-periodic dynamics, which is illustrated by an enlarged fragment of it in Fig.5c. Further transformations and bifurcations with decreasing coupling in the projection onto the variable of the generator of quasi-periodic oscillations do not differ. However, in the projection onto the variable of the Rössler system in Fig. 5b, the doubling points of the three-frequency torus DT_1 and DT_2 are traced.

Since system (3) demonstrates three-frequency tori, it is not enough to use the traditional Poincaré section for its analysis, but the so-called double Poincaré section should be applied. The procedure for its construction is implemented as follows. Using the Hénon method, we find points in the map formed by the cutting hypersurface $y_1=0$, and then select some layer 2×10^{-2} in the vicinity of the hypersurface defining the second Poincaré section $x_2=0$. The points located inside this layer represent the double Poincaré map. Figures 5d and 5e show portraits of attractors in the double Poincaré section. In Fig.5d one can see an invariant curve illustrating the existence of a three-frequency torus. Fig. 5e shows the doubling of the three-frequency torus with a decrease in the coupling strength.

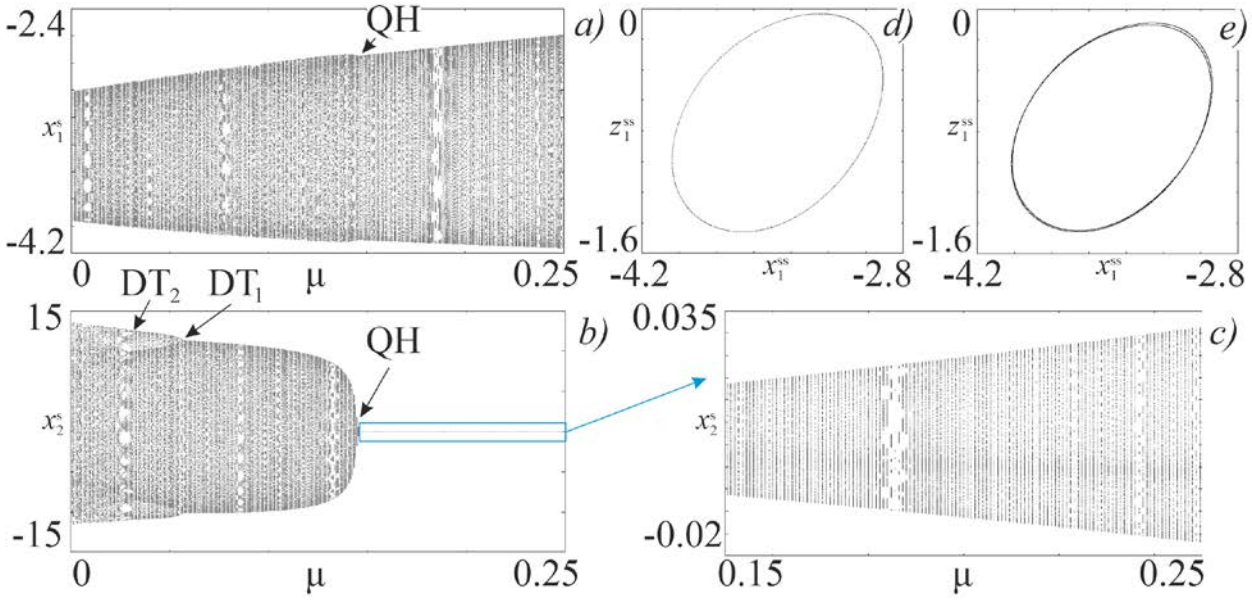

Fig.5. A bifurcation tree in the Poincaré section by a hypersurface $y_1=0$ in projection onto a variable of the first (*a*) and second (*b,c*) subsystems. Poincaré map in the double Poincaré section ($y_1=0$, $|x_2|<10^{-2}$); μ=0.06 (*d*), μ=0.04 (*e*).

3.3. Two-parameter Lyapunov analysis

Let us now carry out a two-parameter analysis, including the region of stronger coupling. Figure 6a shows Lyapunov exponents chart of system (3) on the plane natural frequency of a quasi-periodic generator - the coupling value of subsystems (ω_0,μ) and its enlarged fragment, Fig.6b. The type of regime is determined by the spectrum of Lyapunov exponents by analogy with [22], the dimension of the invariant torus is determined by the number of zero exponents.

The color palette and the correspondence to the spectrum of Lyapunov exponents are deciphered to the right of the Fig.6a. The initial conditions were chosen fixed at each point of the parameter plane.

Figure 6a visualizes the regions of periodic regimes P, two-frequency tori 2T, three-frequency tori 3T, and chaos C. There is also a region in which the system has a stable equilibrium state. The latter is a demonstration of the effect of the oscillations death OD [1] (the term *amplitude death* is sometimes used), when a large dissipative coupling makes an unstable equilibrium stable, thereby inhibiting the oscillations of both oscillators. Note that this effect is of general importance in the theory of coupled systems. It is observed in oscillators of various types, and described in extensive literature, for example [1,53,54].

Note, that in the region of existence of three-frequency tori (see the enlarged fragment, Fig. 6b), one can see lines of doubling bifurcations of such tori DT, on which four Lyapunov exponents vanish $\Lambda_{1,2,3,4}=0$. One can also see narrow regions of three-frequency tori in the area of chaos.

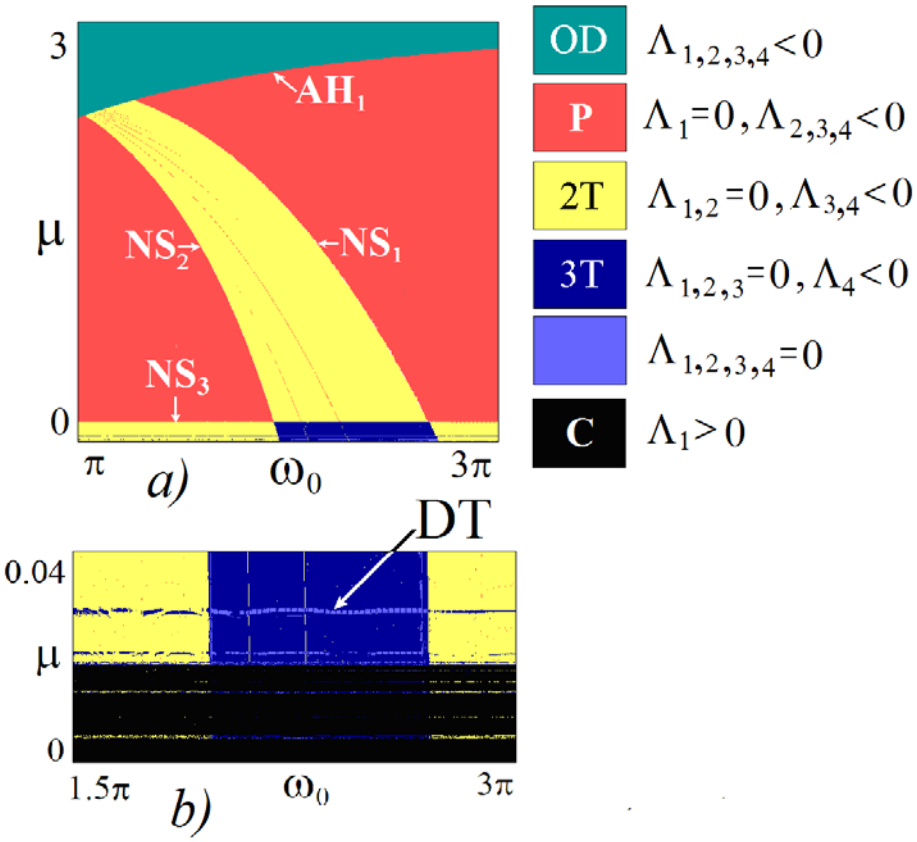

Fig.6. Lyapunov exponents chart of coupled systems (3) (*a*) and its enlarged fragment (b). AH_1 is Andronov-Hopf bifurcation; $NS_{1,2,3}$ is Neimark-Sacker bifurcation; DT is three-frequency torus doubling bifurcation

As we will show below, the region of oscillation death in Fig. 6a borders on the region of periodic regimes along the Andronov-Hopf bifurcation line AH_1, and the region of two-frequency regimes is bounded on both sides by the Neimark-Sacker bifurcation lines of the limit

cycles NS_1 and NS_2. A more subtle picture of bifurcations is observed in a very narrow neighborhood of the line segment in Fig. 6a, in which the oscillation death region visually borders on the quasi-periodicity region. We will give the corresponding analysis below and make a comparison with similar situations known for coupled generators. In the region of small coupling, the boundary of the periodic regime is another Neimark-Sacker bifurcation NS_3.

4. Numerical bifurcation analysis

4.1. One-parameter bifurcation analysis

Let us supplement the above consideration with a bifurcation analysis of equilibrium states and periodic regimes and also specify the character of bifurcations. First, let us consider the case when, as the coupling decreases, a transition is observed from the oscillation death region OD to the region of periodic self-oscillations P. In accordance with Fig. 6a, two options are possible: to the right and to the left of the region of quasi-periodic dynamics. In the first case, we can choose the value $\omega_0 = 5$, and in the second $\omega_0 = \pi$. Fig. 7 shows the appropriate one-parameter bifurcation diagrams over a wide range of coupling strength: $0 \le \mu \le 3$, corresponding to Fig. 6a. The red and black lines show stable and unstable equilibriums, the green line marks stable limit cycles, and the blue and purple lines denote saddle limit cycles (with one- and two-dimension of the unstable manifold, correspondingly). The analysis was carried out using the XPPAUT numerical package [55]. The maximum value of the variable x_1 (x_1^{max}) is plotted on the *y*-axis.

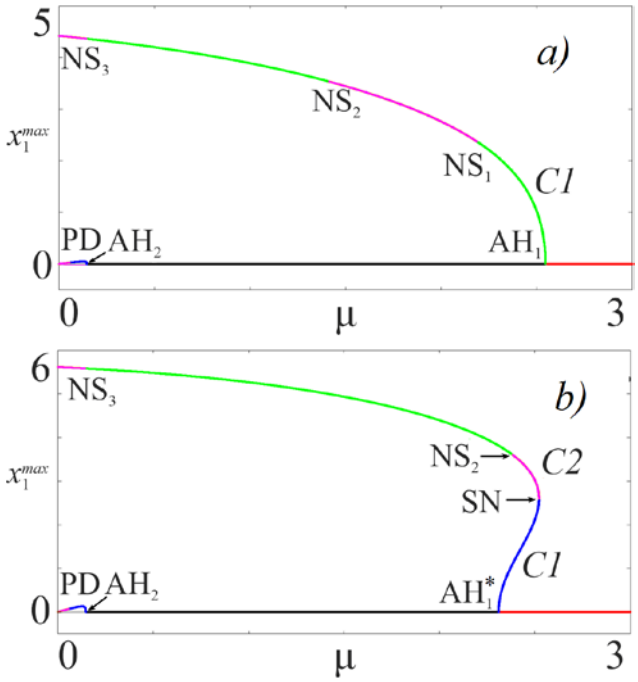

Fig. 7. One-parameter bifurcation diagrams for the transition from the region of oscillation death to the region of periodic oscillations at ω_0=5 (*a*) and ω_0=π (*b*).

In the first case in Fig. 7a, as the coupling value decreases, the equilibrium state undergoes two successive Andronov-Hopf bifurcations. At $\mu\approx2.547$ (AH_1) the equilibrium point loses stability and turns into a saddle-focus with a two-dimensional unstable manifold. Then, at $\mu\approx0.01446$ (AH_2), one more two-dimensional manifold loses stability. Each of the bifurcations is associated with the emergence of a limit cycle. As a result of the first bifurcation (AH_1), a stable limit cycle *C1* is born, which demonstrates three Neimark-Sacker bifurcations with decreasing coupling parameter. The first one occurs at $\mu\approx2.186$ (NS_1), as a result the cycle becomes saddle-focus, and a two-frequency torus is born in its vicinity, which is clearly seen on the chart of Lyapunov exponents in Fig. 6a. A further decrease in the coupling at $\mu\approx1.407$ leads to the Neimark-Sacker bifurcation (NS_2,) passing in the reverse order, which can also be observed on the Lyapunov exponent chart: the regime again becomes periodic. And then, at a lower coupling strength ($\mu\approx0.1445$, NS_3), a two-frequency torus is born again. The second Andronov-Hopf bifurcation AH_2 leads to the birth of a saddle cycle with a one-dimensional unstable manifold, which subsequently undergoes a period doubling bifurcation PD and becomes a saddle cycle with a two-dimensional unstable manifold. Thus, for the given values of the parameter ω_0, the transition from the region of oscillation death to the region of periodic self-oscillations occurs through the classical Andronov-Hopf supercritical bifurcation.

For small values of the parameter ω_0, the transition from the regime of oscillation death to the periodic regime has a more complex bifurcation mechanism, Fig. 7b. As in the first case, the equilibrium state undergoes two successive Andronov-Hopf bifurcations. However, the first bifurcation at $\mu\approx2.31$ (AH_1^*) is subcritical and corresponds to the birth of an unstable (saddle) cycle C*1* with a one-dimensional unstable manifold. This cycle then merges with the C*2* saddle cycle with a two-dimensional unstable manifold as a result of a saddle-node bifurcation at $\mu\approx2.521$ (SN). And further, as the coupling decreases, the second cycle undergoes a Neimark-Sacker bifurcation, which is passed in the reverse order (NS_2, $\mu\approx2.377$), as a result of which the unstable cycle stabilizes. Thus, in this case, the transition from the regime of oscillation death to a periodic one occurs in a hard manner and in a narrow region of the coupling parameter, a stable equilibrium can coexist with a stable torus. For small values of the coupling parameter, similarly to the first case, one can see another Neimark-Sacker bifurcation, where a two-frequency torus ($\mu\approx0.1444$, NS_3) is born.

Let us now discuss the bifurcations on the chart in Fig. 6a appropriate to the transition from the region of oscillation death to the region of quasi-periodicity. Figure 8a shows the corresponding one-parameter bifurcation diagram for $\omega_0=1.2\pi$. The coupling range is chosen as $2.3\le\mu\le2.5$ because the appropriate transition occurs in a narrow region of the coupling parameter. The colors are similar to Fig.7. One can see the following sequence of bifurcations.

With an increase in the coupling at the point of the Andronov-Hopf subcritical bifurcation (AH_1*), the unstable equilibrium becomes stable, and the saddle limit cycle *C1* is born near it. In turn, this cycle at the point of the saddle-node bifurcation SN merges with the stable cycle *C2*. The *C*2 cycle at the point NS_1 undergoes a Neimark-Sacker bifurcation, and as the coupling decreases, a stable torus softly born. Thus, in a narrow interval $2.4 \le \mu \le 2.476$ of the coupling parameter between the points AH_1* and SN, there is a certain transition region, and bistability is possible in the system. In particular, a stable equilibrium can coexist either with a periodic regime or with a stable torus. To the right of the SN point, any oscillations will be suppressed by the coupling. We note that in [22, 56, 57] for coupled generators of different types, a bifurcation was discussed at the boundary of the oscillation death region, as a result of which an attracting two-frequency torus and two saddle limit cycles are born from the equilibrium state in systems identical in control parameters. With the addition of non-identity, however, such a bifurcation was destroyed. In our case, the bifurcation scenario is different, the systems are obviously "non-identical", and the bifurcation structure is stable to some variations of the parameters.

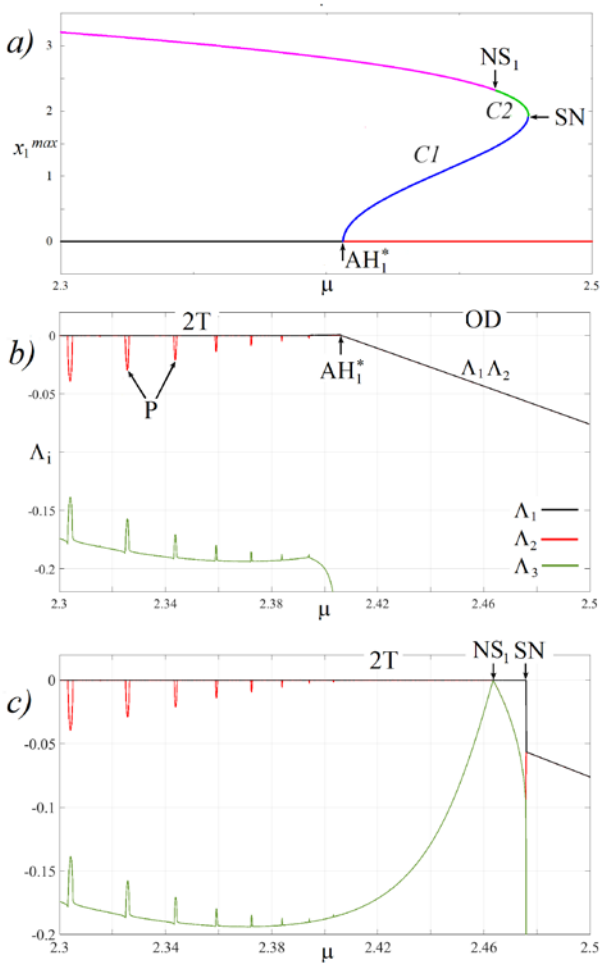

Fig.8. One-parameter bifurcation diagram in the region of transition from the regime of oscillation death OD to quasi-periodicity 2T (*a*) and plots of Lyapunov exponents without inheritance (*b*) and with inheritance (*c*); $\omega_0=1.2\pi$.

It is interesting to compare the bifurcation diagram with the graphs of the Lyapunov exponents and give illustrations of bistability. Different ways of specifying the initial conditions were chosen. Fig. 8b, as in the construction of Lyapunov exponent charts, corresponds to the calculation with fixed initial conditions. At the same time, it is visually indistinguishable from the case of scanning from right to left with "inheritance" of initial conditions, when the initial conditions correspond to the attractor identified in the previous step. Figure 8c corresponds to the calculation with inheritance when scanning along the coupling parameter from left to right. In case (b), to the right of the point AH_1*, the equilibrium state is attractive, and we see two equal negative Lyapunov exponents $\Lambda_1 = \Lambda_2 < 0$ corresponding to this, other exponents are also negative. At the point AH_1* both exponents vanish, the equilibrium becomes unstable, and a hard transition to the torus 2T occurs. In case (c), the graphs visualize the two-frequency torus 2T, which is observed up to the Neimark-Sacker bifurcation point NS_1, at which it turns into a limit cycle. At the saddle-node bifurcation point SN, the limit cycle vanishes. We note that in the domain of existence of the two-frequency torus 2T, the Lyapunov analysis also reveals a set of narrow resonant windows of periodic regimes, two of which are shown by arrows in Fig. 8b and denoted by the letter P.

4.2. Two-parameter bifurcation analysis

Let us now turn to the description of bifurcations on the parameter plane. Figure 9 demonstrates a two-parametric bifurcation diagrams on the plane (ω_0,μ), which are plotted using the XPPAUT package. The scale of Fig. 9a is similar to the chart in Fig. 6a. Figure 9b shows an enlarged fragment. Figure 9a clearly shows that the oscillation death region is bounded by the Andronov-Hopf bifurcation line (AH_1), along which the equilibrium state loses stability with decreasing coupling value. Two lines of Neimark-Sacker bifurcations (NS_1, NS_2) are clearly visible, which on the parameter plane determine the region of two-frequency quasi-periodic oscillations. With a small coupling, the Andronov-Hopf bifurcation line of the saddle equilibrium state (AH_2) and the Neimark-Sacker bifurcation line of the limit cycle (NS_3) of the birth of a two-frequency torus are observed almost simultaneously.

Two-parameter analysis reveals bifurcations of codimension two, which correspond to some points on the parameter plane. Such bifurcations are marked with circles in Fig. 9. The first of them corresponds to the situation when the Andronov-Hopf bifurcation changes character: turns from supercritical AH_1 to subcritical AH_1*. The possibility of both types of this bifurcation was discussed when analyzing one-parameter case. Such a bifurcation is called the Bautin bifurcation (or the degenerate Andronov-Hopf bifurcation) [58] and is indicated in the Fig.9 with label *DAH*.

The line of saddle-node bifurcation of limit cycles SN also comes to the same point, and ends there.

Two more points of codimension two R_1 and R_2 are also marked, where the saddle-node bifurcation line SN and Neimark-Sacker bifurcation lines, respectively NS_1 and NS_2, merge. At that the Neimark-Sacker bifurcation line ends at such a point. These points demarcate the intervals where, as a result of the saddle-node bifurcation, various types of cycles merge. For the values of the parameters ω_0 located to the left of the point R_2, as a result of such a bifurcation, a stable limit cycle and a saddle one merge with a one-dimensional unstable manifold. Between the points R_1 and R_2 on the saddle-node bifurcation line, there is a merging of two saddle cycles, one of which has a two-dimensional unstable manifold. With a decrease in the coupling strength, this cycle is stabilized through the reverse Neimark-Sacker bifurcation. Another saddle cycle has a one-dimensional unstable manifold. This section of the SN line is marked in Fig. 9 by a dotted line. To the right of the point R_1, as a result of the saddle-node bifurcation, the stable limit cycle and the saddle cycle with a one-dimensional unstable manifold again merge.

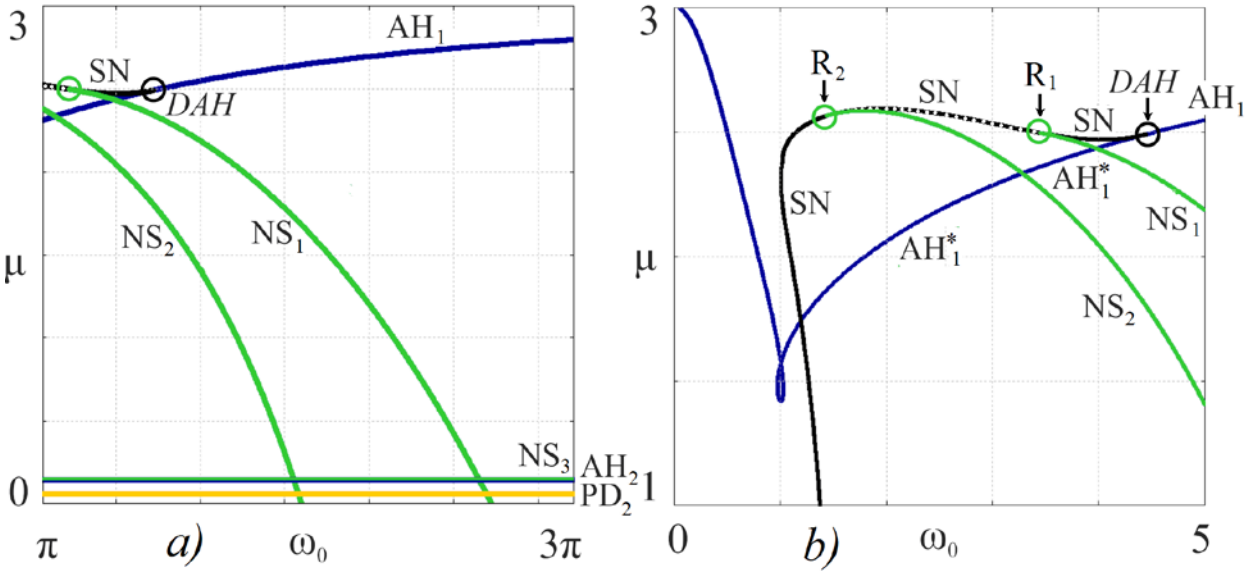

Fig.9. Two-parameter bifurcation diagram and its zoomed fragment for coupled systems (3). AH_1/AH_1* are supercritical/subcritical Andronov-Hopf bifurcations; $NS_{1,2,3}$ are Neimark-Sacker bifurcations; PD_2 is period-doubling bifurcation. Co-dimension 2 points: DAH is degenerate Andronov-Hopf bifurcation (Bautin bifurcation point); R_1, R_2 are resonance 1:1 points

Conclusion

Thus, detailed analysis of the smallest heterogeneous ensemble (interacting models of different types) is presented. Complex behavior in the ensemble characterized for both types of models was revealed.

When a system with an autonomous quasi-periodicity and a chaotic Rössler system interact at a large coupling a regime of oscillation death is observed. As the coupling decreases, periodic self-oscillations and then a two-frequency torus appear. From this torus, as a result of the quasi-periodic Hopf bifurcation, a three-frequency torus is born, undergoing several doubling bifurcations. Further, the three-frequency torus is destroyed, and a kind of chaos with two additional zero Lyapunov exponents is possible (i.e., the total number of zero exponents is three). In the area of chaos, there are narrow regions of existence of three-frequency tori.

The Lyapunov exponent chart makes it possible to reveal the localization of regimes of different types on the parameter plane the natural frequency of a quasi-periodic generator - the value of the coupling of subsystems. The chart is supplemented by bifurcation analysis, which, along with supercritical and subcritical Andronov-Hopf bifurcations, Neimark-Sacker bifurcations and saddle-node limit cycle bifurcations, reveals points of codimension two, in particular, the Bautin bifurcation, in which the supercritical Andronov-Hopf bifurcation turns into a subcritical one.

A new scenario is described for the transition in coupled systems from the regime of oscillation death to quasi-periodicity, which takes place in a certain range of parameters. It consists in the fact that the equilibrium state loses stability through the Andronov-Hopf subcritical bifurcation, colliding with the saddle limit cycle. In turn, this cycle at the point of the saddle-node bifurcation merges with the stable one. The latter undergoes a Neimark-Sacker bifurcation, when a stable torus softly separates from it as the coupling decreases.

Acknowledgment

The research was carried out within the state assignment of Kotel'nikov's Institute of Radio-Engineering and Electronics of Russian Academy of Sciences.

Data Availability

Data supporting numerical experiments presented in this paper are available from the corresponding author upon reasonable request.

Declaration of Competing Interest

Authors declare that they have no conflict of interest.

References

1. Pikovsky A., Rosenblum M., Kurths J. Synchronization: a universal concept in nonlinear science. Cambridge University Press. 2001.

2. Balanov A.G., Janson N.B., Postnov D.E., Sosnovtseva O. Synchronization: from simple to complex. Springer, 2009.
3. Mosekilde E., Maistrenko Y., Postnov D. Chaotic synchronization: applications to living systems. World Scientific, 2002.
4. González-Miranda J.M. Synchronization and control of chaos: an introduction for scientists and engineers. World Scientific, 2004.
5. Anishchenko V.S. et al. Nonlinear dynamics of chaotic and stochastic systems: tutorial and modern developments. Springer Science & Business Media, 2007.
6. Anishchenko V., Astakhov S., Vadivasova T. Phase dynamics of two coupled oscillators under external periodic force. Europhysics Letters. 2009. V. 86. P. 30003.
7. Anishchenko V.S., Astakhov S.V., Vadivasova T.E., Feoktistov A.V. Numerical and experimental study of external synchronization of two-frequency oscillations. Rus. J. Nonlin. Dyn. 2009. Vol. 5, No. 2. P. 237-252
8. Anishchenko V., Nikolaev S., Kurths J. Bifurcational mechanisms of synchronization of a resonant limit cycle on a two-dimensional torus. Chaos: An Interdisciplinary Journal of Nonlinear Science. 2008. V. 18. P. 037123.
9. Emelianova Yu.P., Kuznetsov A.P., Sataev I.R. & Turukina L.V. Synchronization and multi-frequency oscillations in the low-dimensional chain of the self-oscillators. Physica D. 2013. V. 244, no 1. P. 36–49.
10. Emelianova Y.P., Kuznetsov A.P., Turukina L.V., Sataev I.R. & Chernyshov N.Yu. A structure of the oscillation frequencies parameter space for the system of dissipatively coupled oscillators. Communications in Nonlinear Science and Numerical Simulation. 2014. V. 19, no 4. P. 1203–1212.
11. Kuznetsov A. P., Sataev I. R., Turukina L. V. Regional Structure of Two-and Three-Frequency Regimes in a Model of Four Phase Oscillators. International Journal of Bifurcation and Chaos. 2022. Vol. 32, №. 03. P. 2230008.
12. Truong T. Q., Tsubone T., Sekikawa M., Inaba, N. Complicated quasiperiodic oscillations and chaos from driven piecewise-constant circuit: Chenciner bubbles do not necessarily occur via simple phase-locking. Physica D: Nonlinear Phenomena. 2017. V.341. P. 1-9.
13. Truong T. Q., Tsubone, T., Sekikawa M., Inaba N., Endo. Arnol'd resonance webs and Chenciner bubbles from a three-dimensional piecewise-constant hysteresis oscillator. Progress of Theoretical and Experimental Physics. 2017. V. 2017, №. 5. P.053A04.
14. Yoshizawa, T. (2012). Stability theory and the existence of periodic solutions and almost periodic solutions (Vol. 14). Springer Science & Business Media.

15. Arbi A., Tahri N. Stability analysis of inertial neural networks: A case of almost anti-periodic environment. Mathematical Methods in the Applied Sciences, 45(16), pp.10476-10490. (2022).
16. Anishchenko V.S., Nikolaev S.M. Generator of quasi-periodic oscillations featuring two-dimensional torus doubling bifurcations. Technical Physics Letters. 2005. V.31, no.10. P. 853-855.
17. Anishchenko V., Nikolaev S., Kurths J. Peculiarities of synchronization of a resonant limit cycle on a two-dimensional torus. Phys. Rev. E. 2007. V.76, no.4. P. 046216.
18. Anishchenko V., Nikolaev S., Kurths J. Winding number locking on a two-dimensional torus: Synchronization of quasiperiodic motions. Phys. Rev. E. 2006. V. 73. P. 056202.
19. Anishchenko V.S., Nikolaev S.M. Stability, synchronization and destruction of quasiperiodic motions. Rus. J. Nonlin. Dyn. 2006. Vol. 2, No. 3. P. 267-278.
20. Kuznetsov A.P., Stankevich N.V. Autonomous systems with quasiperiodic dynamics examples and their properties: review. Izvestiya VUZ. Applied Nonlinear Dynamics. 2015. Vol. 23, iss. 3. P. 71-93 (in Russian).
21. Kuznetsov A.P., Kuznetsov S.P., Mosekilde E. & Stankevich N.V. Generators of quasiperiodic oscillations with three-dimensional phase space. The European Physical Journal Special Topics. 2013. V. 222, no. 10. P. 2391-2398.
22. Kuznetsov A. P., Kuznetsov S.P., Shchegoleva N.A., Stankevich N.V. Dynamics of coupled generators of quasiperiodic oscillations: Different types of synchronization and other phenomena. Physica D: Nonlinear Phenomena. 2019. V. 398. P. 1-12.
23. Kuznetsov A.P., Sedova Yu.V., Stankevich N.V. Two coupled quasiperiodic generators excited by external harmonic force. Zhurnal Tekhnicheskoy Fiziki. 2021. Vol. 91, №. 11. P. 1619-1624 (in Russian).
24. Stankevich N.V., Kurths J. & Kuznetsov A.P. Forced synchronization of quasiperiodic oscillations. Communications in Nonlinear Science and Numerical Simulation. 2015. V. 20, no. 1. P. 316-323.
25. Kuznetsov A.P., Sedova Yu.V. Anishchenko-Astakhov quasiperiodic generator excited by external harmonic force. Technical Physics Letters. 2022. V. 48, no 2. P. 85.
26. Astakhov S.V., Astakhov O.V., Fadeeva N.S., Astakhov V.V. A ring generator of two- and three-frequency quasiperiodic self-oscillations based on the van der Pol oscillator. Chaos: An Interdisciplinary Journal of Nonlinear Science. 2021. Vol. 31, №. 8. P. 083108.

27. Broer H., Simó C., Vitolo R. The Hopf-saddle-node bifurcation for fixed points of 3D-diffeomorphisms: the Arnol'd resonance web. Bulletin of the Belgian Mathematical Society - Simon Stevin. 2008. Vol. 15, №. 5. P. 769-787.
28. Broer H., Simó C., Vitolo R. Quasi-periodic bifurcations of invariant circles in low-dimensional dissipative dynamical systems. Regular and Chaotic Dynamics. 2011. V. 16, no 1-2. P. 154-184.
29. Kuznetsov Yu. A., Meijer H.G.E. Numerical bifurcation analysis of maps: from theory to software. United Kingdom: Cambridge University Press; 2019.
30. Kamiyama K., Komuro M., Endo T., Aihara K. Classification of bifurcations of quasi-periodic solutions using Lyapunov bundles. Int. J. Bifur. Chaos. 2014. Vol.24, no.12. P.1430034.
31. Komuro M., Kamiyama K., Endo T., Aihara K. Quasi-periodic bifurcations of higher-dimensional tori. Int. J. Bifur. Chaos. 2016. Vol.26, no.07. P.1630016.
32. Sekikawa M., Inaba N. Chaos after Accumulation of Torus Doublings. Int. J. Bifur. Chaos. 2021. Vol.31, no.01. P.2150009.
33. Borkowski L., Stefanski A. Stability of the 3-torus solution in a ring of coupled Duffing oscillators. The European Physical Journal Special Topics. 2020. Vol. 229, №. 12. P. 2249-2259.
34. Gonchenko A. S., Gonchenko S. V., Shilnikov L. P., Towards scenarios of chaos appearance in three-dimensional maps. Rus. J. Nonlin. Dyn. 2012. Vol. 8, no. 1. P. 3-28.
35. Gonchenko A. S., Gonchenko S. V., Turaev D. Doubling of invariant curves and chaos in three-dimensional diffeomorphisms. Chaos: An Interdisciplinary Journal of Nonlinear Science. 2021. Vol. 31, №. 11. P. 113130.
36. Banerjee S., Giaouris D., Missailidis P., Imrayed, O. Local bifurcations of a quasiperiodic orbit. International Journal of Bifurcation and Chaos. 2012. V. 22, №. 12. P. 1250289.
37. Patra M., Banerjee S. Bifurcation of quasiperiodic orbit in a 3D piecewise linear map. International Journal of Bifurcation and Chaos. 2017. V. 27, № 10. P. 1730033.
38. Hidaka S., Inaba, N., Sekikawa,M., Endo T. Hidaka S. Bifurcation analysis of four-frequency quasi-periodic oscillations in a three-coupled delayed logistic map. Physics Letters A. 2015. V. 379, №. 7. P. 664-668.
39. Zhusubaliyev Z.T., Avrutin V., Medvedev A. Doubling of a closed invariant curve in an impulsive Goodwin’s oscillator with delay. Chaos, Solitons and Fractals. 2021. V.153. P. 111571.

40. Anishchenko V.S. Dynamical Chaos: Models and Experiments: Appearance Routes and Structure of Chaos in Simple Dynamical Systems. World Scientific Series on Nonlinear Science. Series A. 1995. V.8.
41. Chua L.O. CNN: A paradigm for complexity. World Scientific. 1998. V. 31.
42. Osipov G.V. et al. Phase synchronization effects in a lattice of nonidentical Rössler oscillators. Physical Review E. 1997. Vol. 55, №. 3. P. 2353.
43. Osipov G.V., Hu, B., Zhou C., Ivanchenko M.V., Kurths, J. Three types of transitions to phase synchronization in coupled chaotic oscillators. Physical Review Letters. 2003. Vol. 91, № 2. P. 024101.
44. Kuznetsov A.P., Migunova N.A., Sataev I. R., Sedova Y. V., Turukina L. V. From chaos to quasi-periodicity. Regular and Chaotic Dynamics. 2015. Vol.20, № 2. P. 189.
45. Pikovsky, A., & Politi, A. (2016). Lyapunov exponents: a tool to explore complex dynamics. Cambridge University Press.
46. Benettin, G., Galgani, L., Giorgilli, A., & Strelcyn, J. M. (1980). Lyapunov characteristic exponents for smooth dynamical systems and for Hamiltonian systems; a method for computing all of them. Part 1: Theory. Meccanica, 15, 9-20.
47. Broer H., Simó C., Vitolo R. Bifurcations and strange attractors in the Lorenz-84 climate model with seasonal forcing. Nonlinearity. 2002. Vol. 15, № 4. P. 1205.
48. Broer H.W., Simó C., Vitolo R. Chaos and quasi-periodicity in diffeomorphisms of the solid torus. Discrete and Continuous Dynamical Systems - B. 2010. Vol. 14, № 3. P. 871.
49. Pikovsky A. S., Feudel U., Kuznetsov S. P. Strange nonchaotic attractors: Dynamics between order and chaos in quasiperiodically forced systems. World Scientific, 2006.
50. Stankevich N.V., Shchegoleva N.A., Sataev I.R., Kuznetsov A.P. Three-dimensional torus breakdown and chaos with two zero Lyapunov exponents in coupled radio-physical generators. Journal of Computational and Nonlinear Dynamics. 2020. Vol. 15, no.11. P. 111001.
51. Grines E. A., Kazakov A., Sataev I. R. On the origin of chaotic attractors with two zero Lyapunov exponents in a system of five biharmonically coupled phase oscillators. Chaos: An Interdisciplinary Journal of Nonlinear Science. 2022. Vol. 32, № 9. P. 093105.
52. Karatetskaia E., Shykhmamedov A., Kazakov A. Shilnikov attractors in three-dimensional orientation-reversing maps. Chaos: An Interdisciplinary Journal of Nonlinear Science. 2021. Vol. 31, № 1. P. 011102.
53. Resmi V., Ambika G., Amritkar R. E. General mechanism for amplitude death in coupled systems. Physical Review E. 2011. Vol. 84, № 4. P. 046212.

54. Saxena G., Prasad A. Ramaswamy R. Amplitude death: The emergence of stationarity in coupled nonlinear systems. Physics Reports. 2012. V. 521, no. 5. P. 205-228.
55. B. Ermentrout. Simulating, analyzing, and animating dynamical systems: a guide to XPPAUT for researchers and students (SIAM, 2002).
56. Ivanchenko M.V. et al. Synchronization of two non-scalar-coupled limit-cycle oscillators. Physica D. 2004. V. 189, no. 1-2. P. 8-30.
57. Astakhov V. et al. Peculiarities of the transitions to synchronization in coupled systems with amplitude death. Chaos: An Interdisciplinary Journal of Nonlinear Science. 2011. Vol. 21, no. 2. P. 023127.
58. Kuznetsov Yu.A. Elements of applied bifurcation theory. New York. Springer. 2004, 3-rd edition.